Supplement of

Constraining Ammonia Emissions in Vehicle Plumes Utilizing Nitrogen Stable Isotopes

Wendell W. Walters[1,2], Linlin Song[3,4,5], Jiajue Chai1[1,2], Yunting Fang[3,4,5], Nadia Colombi[1,*], and Meredith G. Hastings[1,2]

[1] Department of Earth, Environmental, and Planetary Sciences, Brown University, Providence, RI 02912, US
[2] Institute at Brown for Environment and Society, Brown University, Providence, RI 02912, US
[3] CAS Key Laboratory of Forest Ecology and Management, Institute of Applied Ecology, Chinese Academy of Sciences, Shenyang, Liaoning, 110016, China.
[4] Key Laboratory of Stable Isotope Techniques and Applications, Shenyang, Liaoning, 110016, China
[5] College of Sources and Environment, University of Chinese Academy of Sciences, Beijing 100049, China

*Current Address: Department of Earth and Planetary Science, Harvard University, Cambridge, MA 02139, US

Correspondence to: Wendell W. Walters (wendell_walters@brown.edu)

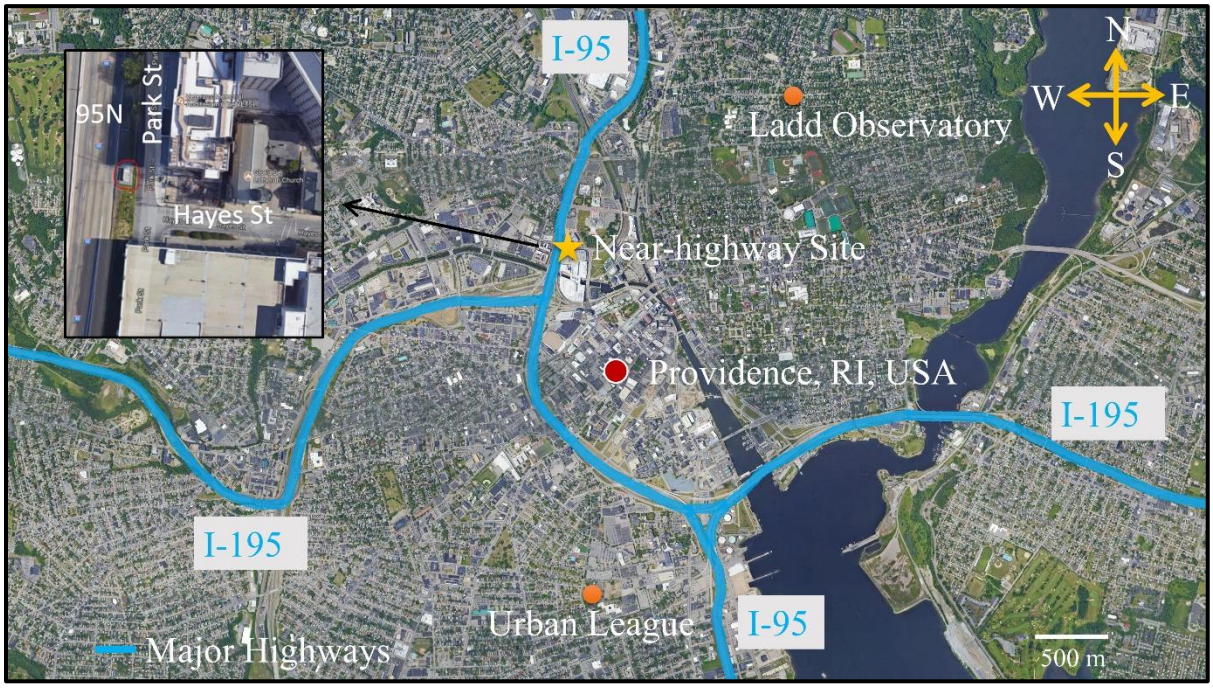

Figure S1: Google Earth image of Providence, RI, US with the locations of the near-highway stationary monitoring site (star), meteorological data monitoring locations (circles), and major interstate highway routes (turquoise). Copyright © 2020 Google.

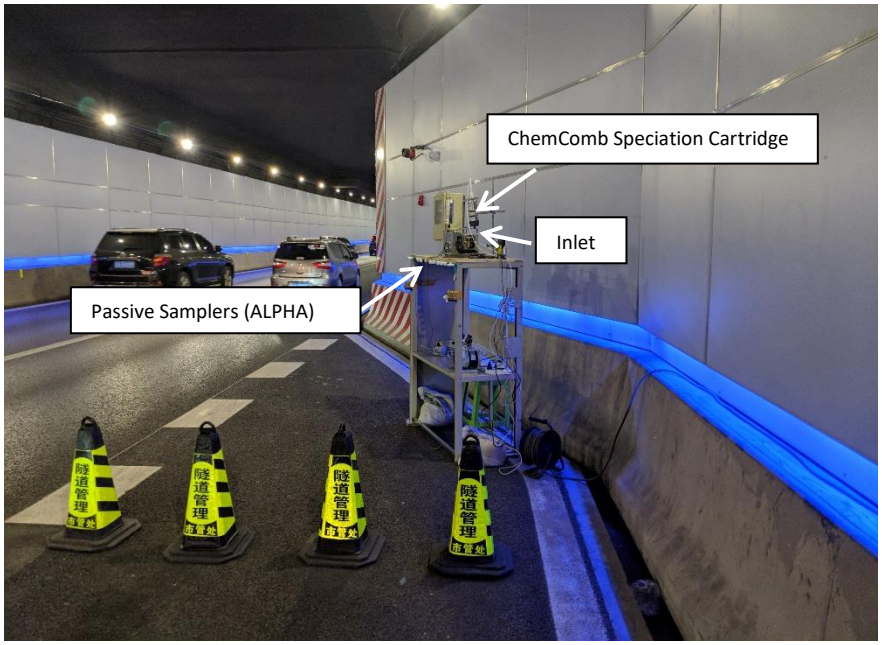

Figure S2: Image of the sampling set-up for collection of NH_3 from fresh vehicle traffic plumes in a tunnel at Shenyang, Liaoning, China.

Figure S3: Image of the mobile lab for on-road collections of NH_3 from fresh vehicle traffic plumes in the northeastern US. The collection of NH_3 was conducted using a ChemComb Speciation Cartridge, which was held in a weatherproof enclosure, and the sampling inlet was directly exposed to ambient air to limit the inlet loss of NH_3.

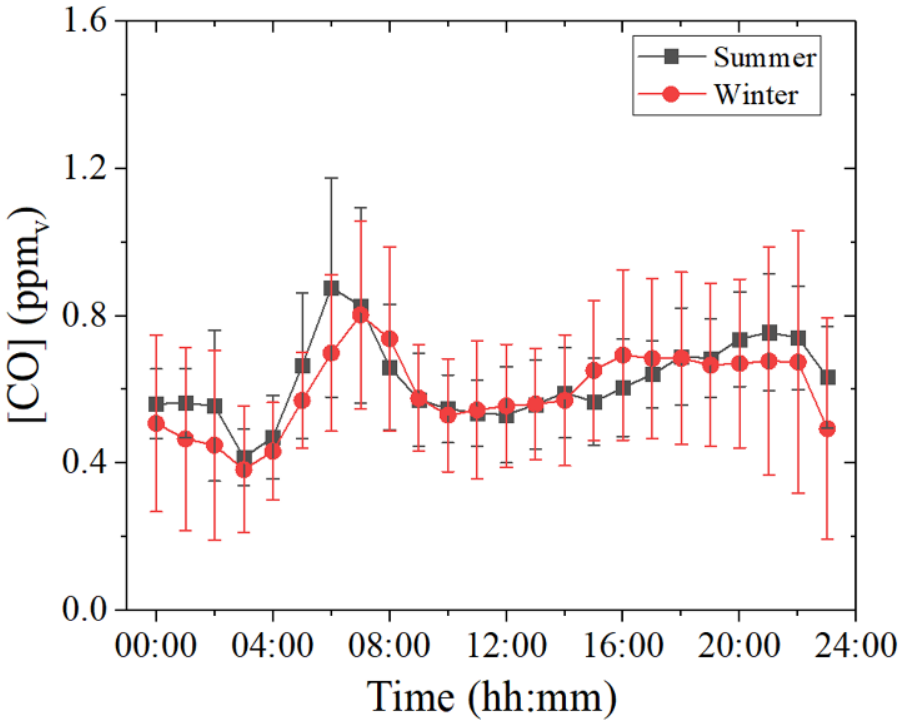

Figure S4: Averaged diel variations in the near highway (Providence, RI, US) [CO] during the summer (August 9 to August 18 in 2017) and winter (January 21 to February 1 in 2018) NH_x collection periods. The data points represent averages for each hour taken from measurements at 5-minute intervals, and the error bars represent ±1σ for each hour.

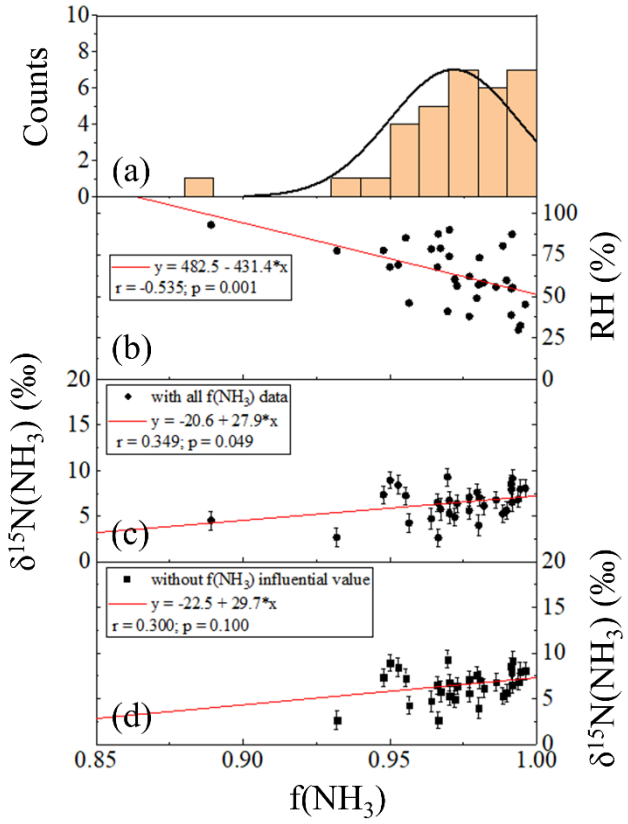

Figure S5: The summer near-highway monitoring (Providence, RI, US) $f(NH_3)$ data including (a) $f(NH_3)$ distribution and linear relations between (b) relative humidity (RH) and $f(NH_3)$, (c) $\delta^{15}N(NH_3)$ and $f(NH_3)$ (all data), and (d) $\delta^{15}N(NH_3)$ and $f(NH_3)$ (without influential $f(NH_3)$ value).

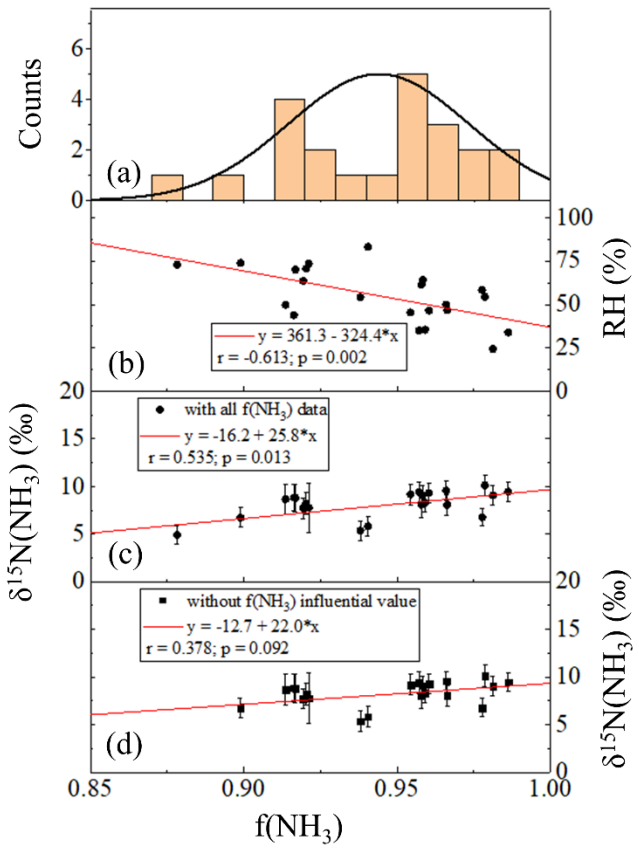

Figure S6: The winter near-highway monitoring (Providence, RI, US) $f(NH_3)$ data including (a) $f(NH_3)$ distribution and linear relations between (b) relative humidity (RH) and $f(NH_3)$, (c) $\delta^{15}N(NH_3)$ and $f(NH_3)$ (all data), and (d) $\delta^{15}N(NH_3)$ and $f(NH_3)$ (without influential $f(NH_3)$ value).

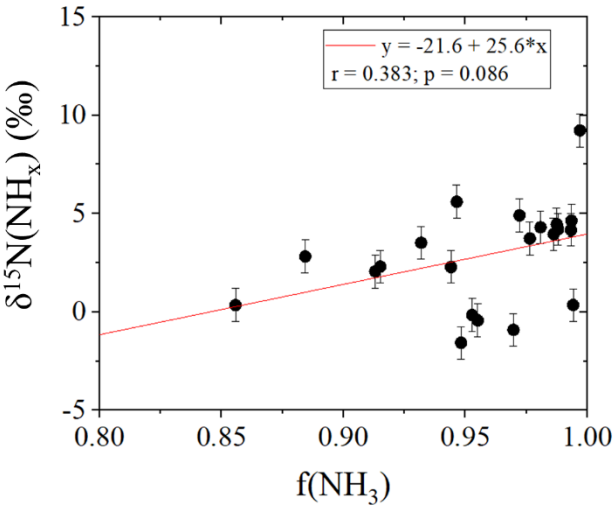

Figure S7: Linear relations at the tunnel monitoring location (Shenyang, Liaoning, China) between $f(NH_3)$ and $\delta^{15}N(NH_x)$.

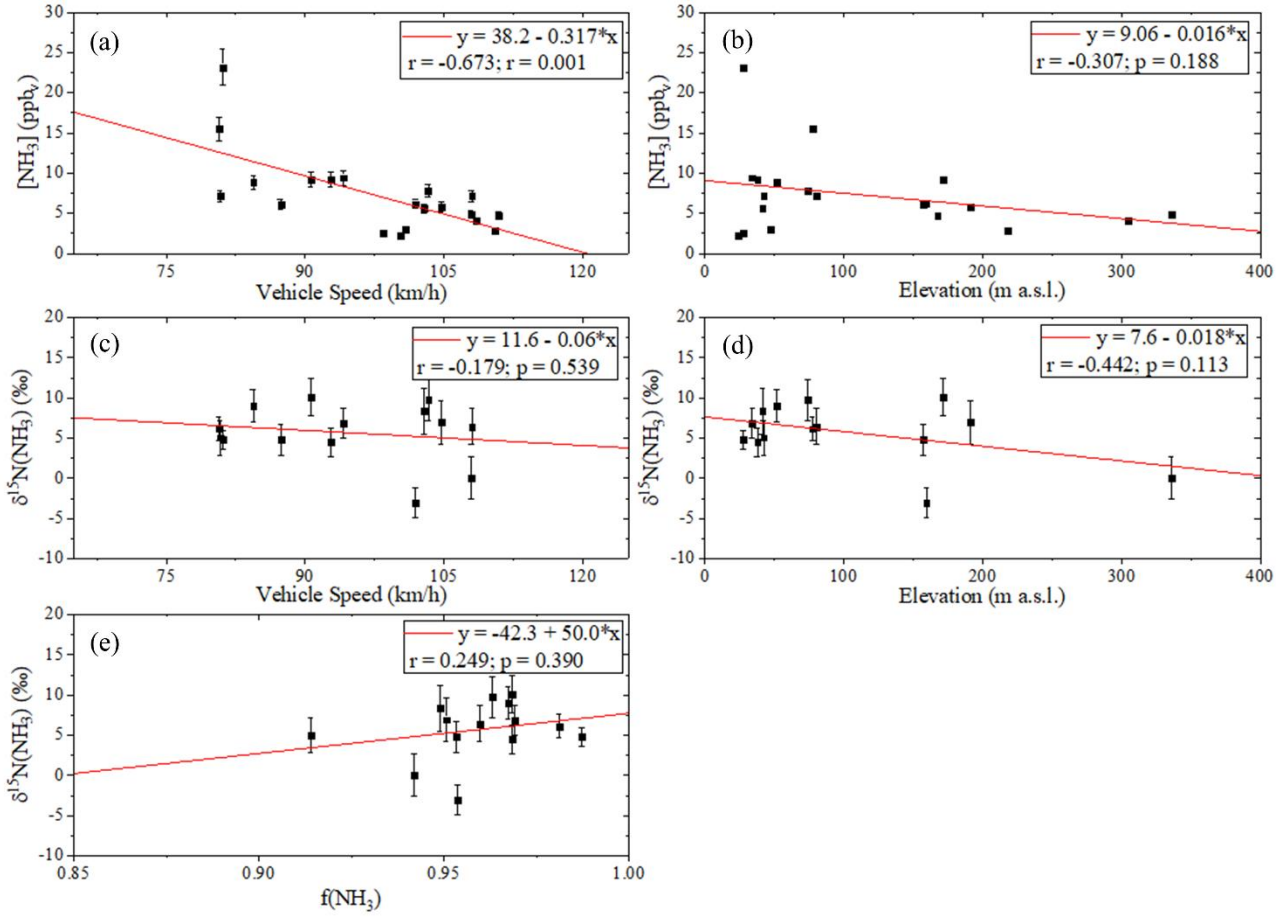

Figure S8: Linear relations from mobile on-road measurements in the northeastern US between (a) $[NH_3]$ and vehicle speed, (b) $[NH_3]$ and elevation, (c) $\delta^{15}N(NH_3)$ and vehicle speed, (d) $\delta^{15}N(NH_3)$ and elevation, and (e) $\delta^{15}N(NH_3)$ and $f(NH_3)$.

Table S1: Summary of the [pNH_4^+] and f(NH_3) data collected at the near-highway monitoring site (Providence, RI, US) during the summer, including the raw measurement and accounting for the potential volatilization of 30% of pNH_4^+ off a denuded PTFE filter.

	Raw Measurement		Accounting for 30% pNH_4^+ Volatilization	
Date	[pNH_4^+] ($\mu g*m^{-3}$)	f(NH_3)	[pNH_4^+] ($\mu g*m^{-3}$)	f(NH_3)
8/9/2017 15:30	0.340	0.977	0.442	0.970
8/9/2017 21:30	0.366	0.973	0.476	0.965
8/10/2017 3:30	0.466	0.932	0.605	0.913
8/10/2017 9:30	0.394	0.972	0.512	0.964
8/10/2017 15:30	0.389	0.957	0.506	0.944
8/10/2017 21:30	0.369	0.966	0.480	0.957
8/11/2017 3:30	0.391	0.966	0.508	0.957
8/11/2017 9:30	0.172	0.982	0.223	0.977
8/12/2017 3:30	0.098	0.994	0.128	0.992
8/11/2017 21:30	0.208	0.986	0.270	0.982
8/12/2017 9:30	0.162	0.967	0.211	0.958
8/12/2017 15:30	0.263	0.981	0.342	0.975
8/12/2017 21:30	0.108	0.992	0.141	0.989
8/13/2017 3:30	0.211	0.970	0.274	0.962
8/13/2017 9:30	0.444	0.953	0.578	0.940
8/13/2017 21:30	0.129	0.991	0.168	0.989
8/14/2017 3:30	0.156	0.988	0.202	0.985
8/14/2017 9:30	0.045	0.992	0.059	0.994
8/14/2017 15:30	0.116	0.991	0.151	0.989
8/14/2017 21:30	0.645	0.948	0.839	0.933
8/15/2017 9:30	0.423	0.970	0.550	0.962
8/15/2017 15:30	0.381	0.977	0.495	0.970
8/15/2017 21:30	0.560	0.955	0.729	0.943
8/16/2017 3:30	0.938	0.889	1.219	0.861
8/16/2017 9:30	0.724	0.950	0.941	0.936
8/16/2017 15:30	0.384	0.970	0.499	0.961
8/16/2017 21:30	0.283	0.980	0.368	0.974
8/17/2017 3:30	0.093	0.980	0.121	0.974
8/17/2017 9:30	0.045	0.996	0.059	0.995
8/17/2017 15:30	0.045	0.994	0.059	0.994
8/17/2017 21:30	0.120	0.990	0.155	0.987
8/18/2017 3:30	0.195	0.964	0.253	0.954
$\bar{x}$	**0.302**	**0.972**	**0.393**	**0.964**
σ	**0.208**	**0.022**	**0.270**	**0.027**

Table S2: Summary of ISORROPIA modeled of NH_x speciation conducted for samples collected in the tunnel from Shenyang, Liaoning, China. Model inputs included [NH_x], [NO_3^T], [SO_4^T], relative humidity (RH) and temperature (Temp) and model outputs included [NH_3] and [pNH_4^+] from which f(NH_3) was calculated. All concentrations are reported in units of μmol*m^{-3}.

	Model Input					Model Output		
Average Collection Date	[NH_x]	[NO_3^T]	[SO_4^T]	RH(%)	Temp (K)	[NH_3]	[pNH_4^+]	f(NH_3)
10/31/18 18:07	7.317	0.041	0.027	39.5	293.1	7.225	0.091	0.987
11/1/18 2:12	3.656	0.065	0.062	33.6	290.4	3.471	0.185	0.949
11/1/18 10:12	5.775	0.157	0.083	32.2	291.0	5.455	0.320	0.945
11/1/18 18:12	9.279	0.000	0.030	31.5	292.7	9.219	0.060	0.994
11/2/18 2:14	3.675	0.063	0.051	36.4	289.5	3.513	0.162	0.956
11/2/18 10:14	7.545	0.324	0.099	37.4	291.6	7.026	0.519	0.931
11/2/18 18:23	9.400	0.388	0.058	37.0	294.9	8.901	0.498	0.947
11/3/18 2:19	3.466	0.363	0.069	41.9	290.4	2.969	0.497	0.857
11/3/18 10:19	6.231	0.381	0.081	36.7	293.1	5.693	0.537	0.914
11/3/18 18:01	7.399	0.413	0.108	40.3	294.1	6.776	0.623	0.916
11/4/18 1:57	4.959	0.352	0.111	45.8	292.1	4.390	0.569	0.885
11/4/18 10:22	4.496	0.034	0.046	41.9	290.9	4.373	0.122	0.973
11/4/18 18:04	9.112	0.026	0.041	44.3	290.2	9.004	0.108	0.988
11/5/18 2:05	3.020	0.035	0.028	30.3	289.8	2.932	0.087	0.971
11/5/18 11:02	6.150	0.047	0.035	27.8	289.6	6.034	0.116	0.981
11/5/18 18:48	7.031	0.041	0.028	24.7	289.9	6.936	0.095	0.986
11/6/18 2:14	2.876	0.056	0.040	20.6	289.7	2.744	0.133	0.954